Chapter 1

Introduction

Creep is a time-dependent deformation that happens when metals or other materials are subjected to stress over a period of time [1]. The applied stress in creep is always less than the yield strength as measured in a tensile test, and yet, creep causes permanent deformation.

Materials such as components of power plant, steam generators or turbine rotors must operate at high temperature, under significant stress. For this reason, the components and structures need to be designed on the basis that excessive creep distortion or creep failure must not occur within the expected operating life of the plant [2]. Knowledge of the creep behaviour of the metals is therefore important, and prediction of creep deformation, i.e. the strain and rupture life, could help to design more reliable parts and components.

1.1 The aim of the work

Creep can be described as a time-dependent and permanent process of materials when subjected to a constant load or stress, which is generally below the yield strength at a certain temperature (usually temperature is greater than approximately 0.4 of the absolute melting temperature $T=0.4T_m$) [3]. Creep deformation can be very large at temperatures around $0.5T_m$.

Creep deformation is normally an undesirable phenomenon, and it is often the limiting factor in the lifetime of a component especially at high temperature and significant stress. In metals, creep usually occurs only at elevated temperatures. Creep at room temperature

is more common in polymeric materials and is called cold flow or deformation under load [4].

The tendency of a material to undergo plastic deformation under the influence of a stress is often characterised using a tensile test, which is in generally conducted under conditions where the measured properties are independent of time [2]. The details on mechanisms of plastic deformation and creep test have been reviewed in a number of excellent publications [5]. The plastic strain is time-dependent in creep deformation. Most creep data are obtained by measuring the deformation of a bar under constant load and temperature over a period of time. The plastic strain on loading is measured as a function of time and a typical variation of creep strain with time for a specimen subjected to a constant tensile stress is shown in Figure 1.1 [6].

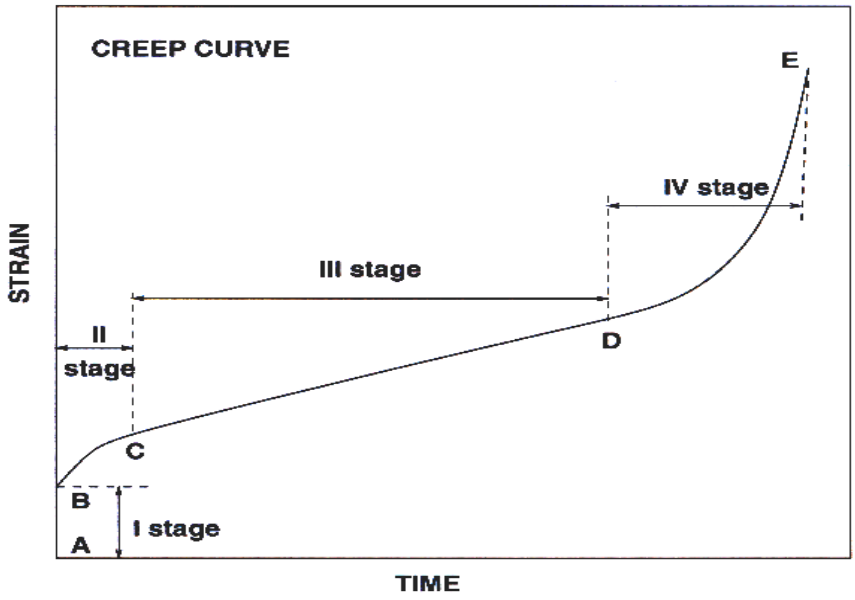

Figure 1.1: General form of strain against time curve. **AB,** elastic extension; **BC**, decreasing creep rate; **CD**, minimum rate of creep; **DE**, increasing creep rate.

As shown in Figure 1.1, the slope of the curve is called creep rate ($\dot{\varepsilon}$) and the end point of the curve **E** is the time for rupture. The creep rate is not ordinarily constant and can be divided into three phases. The region **BC** is commonly considered as primary or transient creep stage [6], and it starts at a rapid rate and slows with time. The region **CD** stands as secondary or steady state creep, which has a relatively uniform rate. **DE** as tertiary creep has an accelerating creep-rate and terminates at the point **E** by failure of material at time for rupture [6].

1.2 Three stages of creep

With the basic definitions and mechanisms of material behaviour explained above, the processes of creep can be subdivided and examined into the three of categories primary creep, tertiary creep, and steady state creep [7]

1.2.1 Primary Creep

During primary creep, the strain rate decreases with time until a constant rate is reached. And this tends to occur over a short period. [8].

Primary creep strain is usually less than one percent of the sum of the elastic, steady state, and primary strains. The mechanism in the primary region is the climb of dislocations that are not pinned in the matrix [7]. Since the amount of initial strain of a material is due to the number of dislocations initially present, the primary region is strongly dependent on the history of the material. If the material has been heavily worked before the creep test, there would be many more dislocations present and the characteristics of the primary creep region would be much different.

1.2.2 Steady State Creep

Steady-state creep is so named because the strain rate is constant. In this region, the rate of strain hardening by dislocations is balanced by the rate of recovery. Steady-state creep is roughly centred at the minimum in the plot of creep rate versus time. The minimum rate is empirically found to be inversely proportional to the time to rupture. This is often called the Monkman-Grant (1956) relationship [9] in which the product of the minimum creep rate and rupture time is found to be constant for a given mechanism.

1.2.3 Tertiary Creep

In the tertiary region, the high strains start to cause necking of the material just as in the uni-axial tensile test. This necking causes an increase in the local stress of the component, which further accelerates the strain [7]. Eventually the material will pull apart in a ductile fracture around defects in the solid. These defects could be precipitates at high temperatures or grain boundaries at lower temperatures [10].

In any case the importance of the tertiary region to normal operation and creep design criteria is minimal. In Figure 1.1 above, the time scale of the tertiary region is greatly expanded for the purpose of clarity. Considering the small amount of time in addition to the fact that the tertiary region develops a plastic instability similar to necking, operating in the tertiary region is not feasible. Therefore it is a conservative estimate to approximate the end of serviceable life of any component to coincide with the end of the steady state creep region. Only under accidental conditions may the extra time in the tertiary region be useful to consider.

The primary creep could be described as the work-hardening stage for the material in which the resistance to creep is built up by virtue of its own deformation; during steady-state creep there is a state of balance between work-hardening and thermal softening; tertiary creep precedes fracture through cavitations, inter-crystalline cracking or some other damage mechanism [11]. The studies on the primary and steady stages of creep are usually more interesting for engineering analysis. Tertiary creep is usually associated with the onset of failure (necking, damage) and is short-lived [11].

Although there are a great number of fundamental theories describing the process of creep deformation and rupture life in different regimes of stress, temperature and strain rate, the theories have not been applied with effect in useful materials of the type used in engineering. This is because practical materials tend to be complex.

1.3 Parametric models

It is very important to understand the long-term creep deformation and its rupture properties of components for their safe use such as power plant and aero-engines [2]. There exist a great number of empirical or semi-empirical methods, which permit the accurate formulation of experimental data and extrapolate long-term creep data. Details of these methods have been reviewed in published literature [12]. For instance, a popular empirical method involving the use of θ-parameter equation was summarized by Evans and Wilshire in 1985 [2, 11]:

$$\varepsilon=\theta_1[1-\exp\{-\theta_2 t\}]+\theta_3[\exp\{\theta_4 t\}-1] \qquad \text{(Eq. 1.1)}$$

where θ_i were obtained by fitting to experimental data, and t is the time at temperature. The first two of these parameters describe the primary or decaying strain rate component, whereas the remaining terms the accelerating regime.

Previous work on prediction of long term creep rupture life of 2.25Cr-1Mo showed that a constitutive creep equation of steady-state stage could predict long-term creep curves [13]:

$$\varepsilon=\varepsilon_0+A\{1-\exp(-\alpha t)\}+B\{\exp(\alpha t)-1\} \qquad \text{(Eq. 1.2)}$$

where ε_0, A, B, α are parameters determined by curve fitting to a measured creep curve. It is almost the same as the θ-parameter method discussed in the previous paragraph. This equation can represent creep curves up to the tertiary creep stage. The parameters are formulated as simple functions of stress and temperature, and they can be extrapolated to long-term creep properties with a lower stress and a lower temperature [13]. Maruyama *et al.* summarized that rupture life was linearly related to the following rupture parameter P derived from the creep equation [14, 15]:

$$P=(1/\alpha)\ \ln\{(\varepsilon_r-\varepsilon_0-A)/B\} \qquad \text{(Eq. 1.3)}$$

where ε_r is the strain to rupture. The long-term creep rupture life could be predicted with the aid of the parameter P. And the prediction of creep curves and rupture life were confirmed by long-term creep tests [13].

However, the parametric models are not sufficiently general to deal with large numbers of variables although they have been applied widely. An artificial technique, the neural network method, has shown superior ability in extrapolation of long-term creep properties. And it is the most general method for empirical representation of creep data.

Chapter 2

Neural Network Model

2.1 Neural Networks

A neural network is a general statistical method of regression analysis, in which a very flexible non-linear function can be fitted to the experimental data. And a neural network model can be used to perform empirical regression [16]. The details of neural networks have been extensively reviewed in many references [17, 18]. The artificial neural network can overcome some difficulties associated with general linear regression in which one must choose an exact relationship between the parameters before the analysis started. It can therefore arrive at the mathematical model without prior assumptions about the form of the relationships [19].

Generally speaking, a neural network model is built by adjusting a set of fitting parameters known as weights, and the weights make up a model, which represents a mapping from the input values to the output values [20]. The weights are calculated by passing examples of input-output pairs through the model in order to minimise a carefully constructed error function [21]. A potential difficulty with using the non-linear regression methods is the possibility of over-fitting data. Using Bayesian methods to control model complexity can solve the over-fitting problem [16]. However, the weights may not always be easy to interpret. For instance, there may exist more than just pair-wise interactions, in which case the problem becomes more difficult to visualize from an examination of the weights [12]. A better method is to actually use the network to make predictions and to see how these depend on various combinations of inputs [22].

The flexibility of the non-linear function is related to the number of hidden nodes i. The final output y (dependent variable) is defined as below [22]:

$$y = \sum_i w_i^{(2)} h_i + \theta^{(2)} \qquad \text{(Eq. 2.1)}$$

where

$$h_i = \tanh\left(\sum_j w_{ij}^{(1)} x_j + \theta_i^{(1)} \right) \qquad \text{(Eq. 2.2)}$$

where x_j are variables on which the output y depends, w_i are weights, and θ_t the biases. They are treated internally as weights associated with a constant input set to unity. A hyperbolic tangent function is used because such a function is non-linear and flexible in the sense that its shape is dependent on weights [16]. Combining several hyperbolic tangents together gives greater flexibility so that the complexity of the model is related to the number of hyperbolic tangent operators used. Given the functions and weights, the minimum and maximum values of the input variables define the network completely [22]. Note that the complexity of the function is related to the number of hidden units. The availability of a sufficiently complex and flexible function means that the analysis is not as restricted as in linear regression where the form of the equation has to be defined explicitly before the analysis [17].

The neural network can capture interactions between the input variables because of the non-linear hidden units have excellent flexibility [21]. However it is also possible to discover more complex relationships in data than the traditional linear regression method. In this case, the over-fitting will unavoidably appear in the model, which means a neural network model that fits the training data well may exist, but it will generalize the test data

poorly. To solve this problem, Mackay discovered that a Bayesian regularization theory can be used to control the complexity of the neural network model [16, 19]. And the Bayesian neural network method, by avoiding over-fitting, can also automatically identify which of many possibly relevant input variables are actually significant factors for the non-linear regression [16].

When the neural network is trained on empirical data, the parameters are adjusted so as to produce a non-linear function that fits the data well. The outcome of training is a set of coefficients and a specification of the functions, which include the weights relating the input to the output [17]. The training process involves a search for the optimum non-linear function between the inputs and the outputs, and is computer intensive. Once the network is trained, the estimation of the outputs for any given inputs is very rapid [18].

On the basis of the trained and tested neural network creep strain model, predictions of creep strain against each of the input variables such as time, temperature, and stress could be made. And the error bars of the predictions quantify the certainty about its predictions.

2.2 Hybrid procedure of modelling

There are a lot of empirical equations for modelling and extrapolating creep strain. For example, the θ-parameter method has been discussed in previous section. Neural network model is the most general method for the empirical representation of creep properties [2]. Although empirical equations have been generally applied, a potential difficulty in predicting creep strain and rupture life with empirical models is that they do not deal with large number of variables and have no firm physical basis. This explains why most of the

empirical approaches are restricted to limited ranges of compositions and types of creep mechanisms.

On the other hand, physical models can describe creep strain with few arbitrary parameters (in terms of stress, temperature and time, etc.), and predictions made by physical models can be verified or disproved. This work presented here is a hybrid procedure in which a neural network model was created with inputs determined by the physical formulations of the simple creep theory, thereby combining the best of both empirical representations and physical models. It aims at predicting long-term creep strain and its dependence on stress, temperature, etc.

Chapter 3

Modelling of Creep Strain

3.1 Constitutive Creep equations

Bhadeshia [12] had summarised the steady-state creep strain rate as a function of the applied stress (σ), the absolute temperature T, and the grain size (d) :

$$\dot{\varepsilon} = f\{\sigma,\ T,\ d\} \qquad \text{(Eq. 3.1)}$$

or more explicitly as [23]

$$\dot{\varepsilon} = \alpha_1 \left(\frac{DGb}{kT}\right)\left(\frac{b}{d}\right)^m \left(\frac{\sigma}{G}\right)^n \qquad \text{(Eq. 3.2)}$$

where a_1 is usually an empirical constant, D is an appropriate diffusion coefficient, b is the magnitude of the Burgers vector and G is the shear modulus. The stress-exponent n and the grain size exponent m are dependent on the mechanism of creep. And the diffusion coefficient D in ferrite can be expressed as below [24].

$$D = D_0 \exp\left(-\frac{Q}{RT}\right) \qquad \text{(Eq. 3.3)}$$

where D_0 is the pre-exponential term in diffusion coefficient, Q is the activation energy [25]; R is the real gas law constant. The equation of creep strain can therefore be expressed as below:

$$\varepsilon = \alpha_1 \left(\frac{DGb}{kT}\right)\left(\frac{b}{d}\right)^m \left(\frac{\sigma}{G}\right)^n t \qquad \text{(Eq. 3.4)}$$

In this physical creep strain equation, variables $\frac{1}{T}$, ln(T), $\ln\left(\frac{\sigma}{G}\right)$, ln($t$) are four inputs in the neural network model, and ln(ε) is the output variable.

3.2 Physical input variables for neural networks

A neural network within a Bayesian framework is used to estimate creep rate of 2.25Cr-1Mo steels. This technique not only reproduces correctly known influence of creep stress, temperature, time and chemical compositions, but also grasps the interactions between different parameters.

3.2.1 The logarithm of the constitutive creep equation

Since there are two exponents in the creep strain constitutive equations (Eq. 3.4), in the database of neural network model, the output variable creep strain ε would be replaced by ln(ε) in order to find out more accurate predictions on creep strain ε and its dependent physical inputs. A function of creep strain could be expressed as below:

$$\ln(\varepsilon)=n\ln\left(\frac{\sigma}{G}\right)+\ln\left(\frac{Gb}{k}\right)+\ln D_0-\frac{Q}{RT}-\ln T+m\ln\left(\frac{b}{d}\right)+\ln t \qquad \text{(Eq. 3.5)}$$

It would be possible to improve the prediction of the creep strain by changing the input variables to the inverse of the absolute temperature ($\frac{1}{T}$), the natural logarithm values of creep time (ln$t$), the temperature (ln$T$) and $\ln\left(\frac{\sigma}{G}\right)$ respectively. Changing the inputs in terms of the natural logarithm could help a lot to get more sensible graphs of ln(ε) on its dependent inputs. In Equation 3.5, $\ln\left(\frac{\sigma}{G}\right)$, ln$t$, $\frac{1}{T}$, ln$T$ are four important variables on which the creep strain ln(ε) depends on.

3.2.2 Heat treatment conditions and compositions of 2.25Cr-1Mo steels

Besides those four variables, heat treatment, and main chemical compositions of several different experimental 2.25Cr-1Mo steels were also necessary input variables for an artificial neural network model [22].

Steel	2.25Cr-1Mo
Normalising temperature /K	1203
Duration / h	6
Cooling rate	water quenched
Tempering temperature / K	908
Duration / h	6
Cooling rate	air cooled
Annealing temperature / K	873
Duration / h	2
Cooling rate	air cooled
Composition	
C wt%	0.15
Si	0.21
Mn	0.53
P	0.012
S	0.012
Cr	2.4
Mo	1.01
Ni	0.014
Al	0.018
B	0.0003
Co	0.05
Cu	0.16
N	0.0108
Nb	0.005
V	0.01
W	0.01
Re	0.0003
Ta	0.0003

Table 1. Heat treatment and chemical composition of 2.25Cr-1Mo steel [22].

3.2.3 Detailed chemical analysis of 7 different steels of 2.25Cr-1Mo (wt %)

Data of chemical compositions were from NRIM datasheet [26] and published literatures. Information on compositions of each steel varied because it was collected from various sources. And the steel reference codes from literatures [27] are W1413, W1414, W1417, W1420, W1473 and W1486 respectively. The NRIM reference code of normalized and tempered 2.25Cr-1Mo steel plates was MaC.

Steel Code	Composition (wt%)								
	C	Si	Mn	S	P	Ni	Cr	Mo	Al
W1413	0.08	0.17	0.78	0.009	0.021	0.18	2.91	0.99	0.011
W1414	0.08	0.16	0.79	0.009	0.021	0.17	2.85	0.98	0.011
W1417	0.08	0.16	0.82	0.009	0.018	0.17	2.91	0.98	0.012
W1420	0.08	0.15	0.79	0.008	0.009	0.17	2.89	0.99	0.012
W1473	0.09	0.16	0.88	0.011	0.015	0.17	2.96	0.97	0.001
W1486	0.07	0.17	0.89	0.011	0.015	0.17	3.02	0.98	0.002
MaC	0.12	0.29	0.48	0.007	0.015	0.05	2.20	0.99	0.017

Table 2. Detailed chemical analysis of 7 different steel of 2.25Cr-1Mo (wt %) [26].

The chemical composition data for some of the steels were incomplete, especially with respect to some of the trace impurity elements (such as Sn, Ti, Co, As, Nb, Zr, B etc.). It would probably mislead the neural network analysis by assuming the missing impurity elements were at zero concentration. Therefore, these impurity elements were assumed to have values given by the mean concentration in each case. By contrast, for the major

chemical composition elements (C, Si, Mn, S, P, Ni, Cr, Mo, Al), compositions were set to the exact data listed in Table 2 for various steels.

3.3 Extrapolation of shear modulus

The value of the shear modulus for pure iron is $G=8.065\times10^{10}\mathrm{N/m^2}$ [28, 29]. Early experimental works of Speich, *et al.* [30] had summarized that both the Young 's modulus (E) and shear modulus (G) of isotropic Fe and binary Fe-C, Fe-Co, Fe-Cr, Fe-Ir, Fe-Ni, Fe-Pt, Fe-Re, Fe-Rh, and Fe-Ru alloys had been determined as functions of composition and temperature (77 to 473 K) by a pulse-echo technique (100 kHz elastic waves). To prepare the input variables datasheet for the neural network model, the shear modulus G should be extrapolated as a function of temperature. The temperature dependence of shear modulus G for iron and a number of the binary alloys were given in Figure 3.1 [30]. The shear modulus G decreases in a non-linear manner between 77 and 473 K. At this stage, the influence of the chemical compositions to the shear modulus may be neglected, and a simple neural network could extrapolate the shear modulus $G=f(T)$ as a function of temperature ranging from 477 to 1000 K.

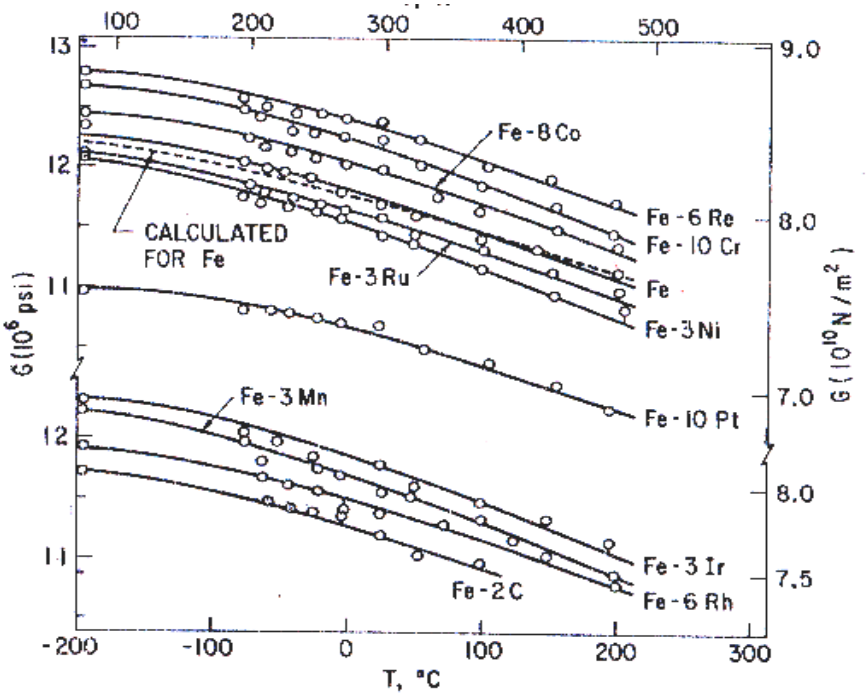

Fig 3.1 The temperature dependence of shear modulus *G* for iron and a number of the binary alloys [30].

The data of shear modulus and temperature were collected by digitizing the plot of shear modulus as it varied with the temperature for the pure iron (Figure 3.1) with the help of DATA Thief software. As the data were based on extrapolation from a larger number of alloys, all of which were substantially isotropic, they were believed to represent more truly polycrystalline isotropic iron. And the database of neural network model was prepared in which the temperature *T* was the input variable and the shear modulus *G* was the output. Since there were only one input variable and one output, a simple neural network model was trained and tested, and an equation of shear modulus had been extrapolated:

$$G=-1.08\times10^{-3}\times T+8.87 \qquad \text{(Eq. 3.6)}$$

where *T* is the temperature (K) and the unit of shear modulus *G* is ($\times10^{10}$ N/m^2)

3.4 Building a database

In order to build a neural network model, the first step was to prepare a database, which was compiled for the creep data of various kinds of 2.25Cr-1Mo steels. When training a model, the selection of input variables is very important as well as the specific combination of these variables. In order to predict the non-linear relationship between the strain ε and dependence, variables $\frac{1}{T}$, ln(T), ln($\frac{\sigma}{G}$), ln(t) would be selected as the inputs instead of the test conditions themselves (stress σ and temperature T, creep time t).

There were 14 input variables in the whole database including the chemical compositions of the test steels and the heat treatment conditions. The conditions of heat treatment for the various 2.25Cr-1Mo steels are different, which is obviously shown in Table 3 [26, 27].

Reference code	Heat treatment
W1413/W1414	1233K/8h Air cool 973K/12h Furnace cool
W1417/W1420 W1473/W1486	973K/12h Furnace cool
MaC	1203K/1h Air cool 1013K/2h Air cool 973K/4h Furnace cool

Table 3. Different heat treatment conditions of various 2.25Cr-1Mo steels [26, 27].

In the preparation of the database for the neural network model, the raw information of heat treatment conditions had to be converted into a form suitable for the neural network analysis. Three heat treatment (each characterised by a temperature, duration, and cooling rate from the treatment temperature) would be differentiated with three simple numbers

1, 2, 3, which was shown in Table 4. The output variable was ln(ε) and the minimum and maximum values were given in Table 4.

Input variables	Minimum	Maximum	Mean	Std deviation
$1/T$ (K^{-1})	0.0012	0.0015	0.0013	0.0001
ln(T) (K^{-1})	6.517	6.7130	6.683	0.0469
ln(σ/G)	-7.8859	-5.4919	-6.7513	0.7483
ln(t) (h)	0.6931	11.3908	6.6509	2.31
Heat treatment	1.0000	3.0000	2.02115	0.74
C wt%	0.07	0.12	0.0963	0.02
Si	0.15	0.29	0.2134	0.635
Mn	0.48	0.89	0.6849	0.1727
S	0.007	0.01	0.0085	0.0015
P	0.009	0.02	0.0157	0.0034
Ni	0.05	0.18	0.1228	0.0602
Cr	2.20	3.02	2.6319	0.3588
Mo	0.97	0.99	0.9854	0.0069
Al	0.001	0.017	0.0117	0.0057
ln(ε)	-7.6009	-2.9957	-5.6123	1.4157

Table 4. The variables involved in the neural network analysis

It is impracticable to provide comprehensive creep data in the database, because some creep deformation has to be predicted for very long times (greater than 200,000h in some cases); and at the same time, creep strain data are generally kept secret for commercial reasons. Therefore, it was decided to focus on 2.25Cr-1Mo steel, which is a very well established alloy, and for which there are a few creep data available in the literature.

3.5 Creep strain model with physical inputs

Data from published literature were collected in a database, and all the data of input variables were randomized and split into a training set and a testing set [20]. All the 14 input variables and the output variable were first normalized within the range ± 0.5 according to:

$$x_N = \frac{x - x_{\min}}{x_{\max} - x_{\min}} - 0.5 \qquad \text{(Eq. 3.7)}$$

where x is the original value from the database, $x_{\max}$ and $x_{\min}$ are the maximum and minimum of each variable in the original data, and x_N is the normalized value [22]. The step of normalization variables was not significant for running the neural network model but it allows a convenient way to compare the results of the output [22]. The minimum and maximum of each variable and the target were searched, and the information was stored in the data file of MINMAX.

3.5.1 σ_v, LPE, TE plots of creep strain model

About 86 sub-models have been trained successfully and 20 sub-models have been tested to build a committee. These sub-models were different from one another in the initial number of hidden units and starting weight values. For several runs of the neural network model, Figure 3.2 (a) showed the model perceived noise σ_v as a function of the number of hidden units in the creep strain model. As expected, σ_v decreased as the fitting function became more flexible with the large number of hidden units. On the other hand, Figure 3.2 (b) showed that the test error at first decreased and then nearly levelled out,

with minima appearing between 18 and 20 hidden units. The log predictive error (LPE) was used to evaluate the performances of different models [31].

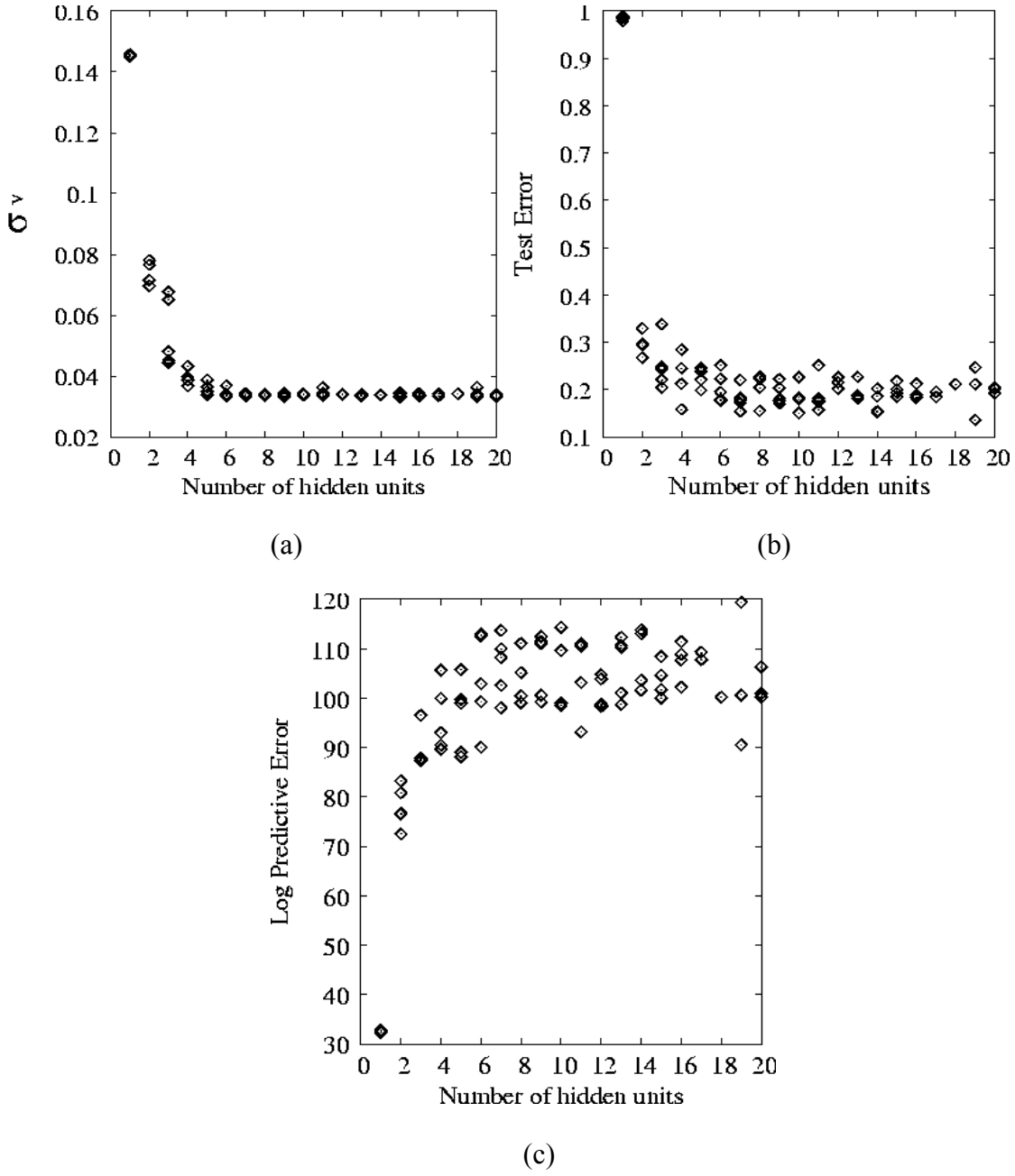

Figure 3.2: The perceived level of noise σ_v (a), the test error (b), the log predictive error (c) of models with increasing numbers of hidden units.

Figure 3.3 compares the predicted values with the actual values for the best model, consisting of 20 hidden units, using the split database. The comparison of training database (seen data) with the model showed good agreement as should be expected Figure 3.3 (a) The analysis of testing database (unseen data) by the physical strain model also showed agreement (b).

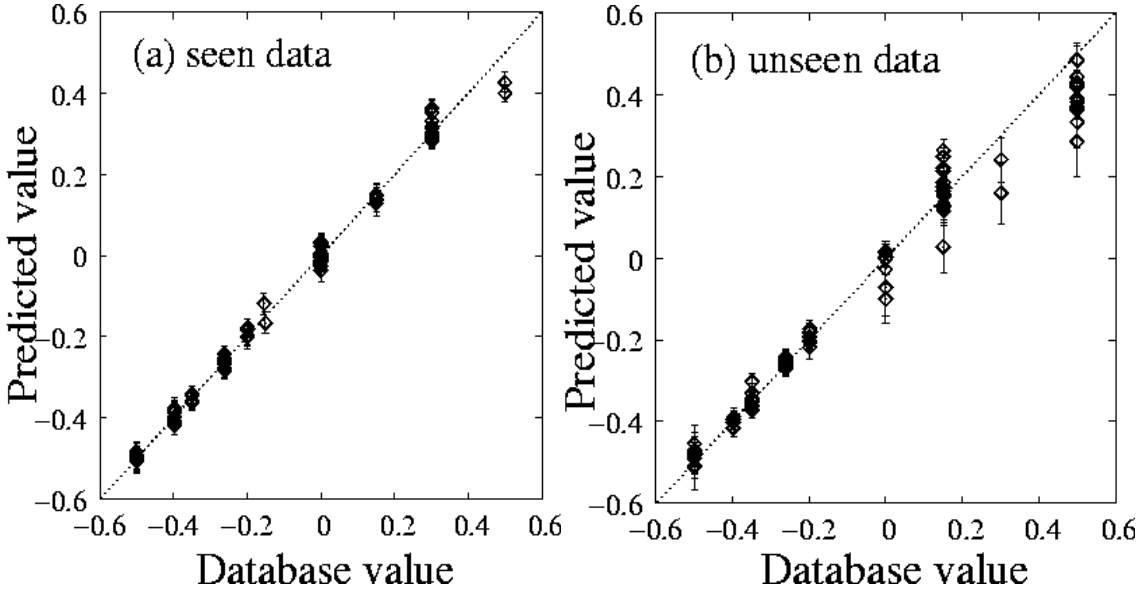

Figure 3.3 Comparison of predicted versus actual creep strains for the training set (a) and testing set (b), using the best model.

3.5.2 Committee of the trained models

The purpose and methods for building a committee model has been discussed in a lot of the reference [17, 18, 32]. In real data analysis situation, no single model will completely capture the true relationship between the inputs and outputs. Using a committee of sub-models rather than only one sub-model can improve predictions of the creep strain model in regions where there is great uncertainty. Committees of sub-models were formed with the best prediction models, and the best models were ranked using the

values of the test errors. To do this, a given number of sub-models was considered and predicted on the second half of the database (the unseen data) to calculate the combined test error.

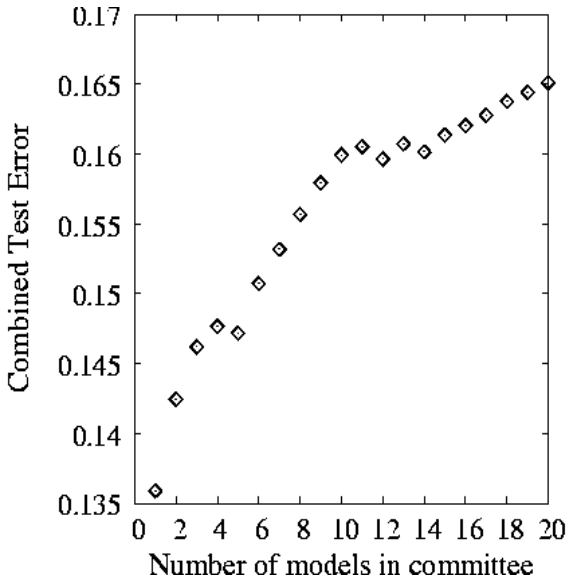

Figure 3.4 The combined test error for the optimum model committee suggested by neural network.

After the sub-models had been trained, a plot of the test error of the committee versus the number of models in the committee gives a minimum which defines the optimum size of the committee, as shown in Figure 3.4. The test error associated with the best single model is clearly greater than that of any of the committees. It was determined in the present case that a committee of only one model would be the best choice, being the committee of the lowest test error. The committee was then retrained on the entire data set without changing the complexity of any of its members. The tested sub-models were ranked with the decreasing orders of Log Predictive Error (LPE) values. In this creep strain model, the optimum committee was suggested to have only one member with the

largest value of LPE (LPE=119.44 for the sub-model "_rs5"), and the minimum test error would be equal to 0.1359.

3.5.3 Perceived significance bar chart

The perceived significance parameter σ_w indicated the importance of an input variable in terms of its variation having an effect on the output of the model. Figure 3.3 compared values of σ_w for a selection of input variables for the optimum model committee. A high value of σ_w for a specific input variable can be caused by the corresponding variable inducing a large variation in the output.

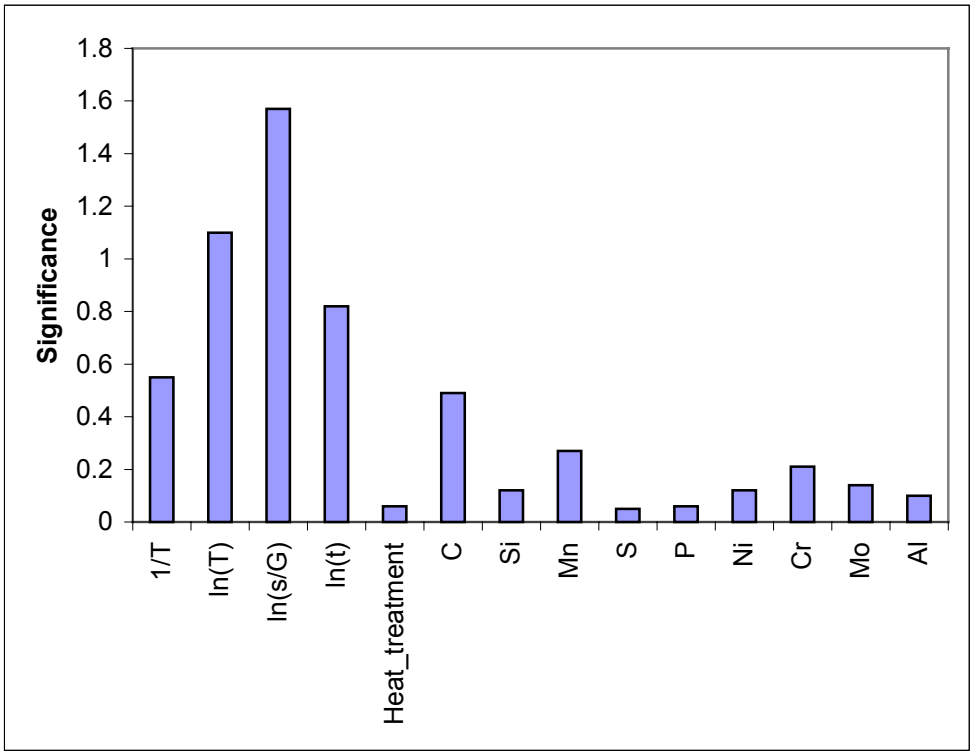

Figure 3.4 The perceived significances parameter σ_w for input variables of the optimum model committee.

As the bar chart of perceived significance value σ_w shows (Figure 3.4), the five input variables with largest σ_w are the most important inputs for the output of the model. They were $\frac{1}{T}$, ln(T), ln($\frac{\sigma}{G}$), ln(t) and the composition of carbon C wt% in the 2.25Cr-1Mo steels respectively. The other nine input variables with very small values of perceived significance σ_w, including the heat treatment conditions for the steel, did not have strong influence on the output ln(ε), and predictions of these variables and detailed analysis of their influence would be neglected.

3.6 Completely empirical neural network model

There was another way to build a completely empirical neural network model, in which case all the inputs were directly from the published literature on creep strain.

Input variables	Minimum	Maximum	Mean	Std deviation
σ (MPa)	20.0	333.0	116.50	87.2830
T (K)	673.000	823.0000	799.6025	36.3317
t (h)	2.0000	88500.00	5036.394	11602.27
C wt%	0.0700	0.1200	0.0963	0.0200
Si	0.15	0.29	0.2134	0.635
Mn	0.48	0.89	0.6849	0.1727
S	0.007	0.01	0.0085	0.0015
P	0.009	0.02	0.0157	0.0034
Ni	0.05	0.18	0.1228	0.0602
Cr	2.20	3.02	2.6319	0.3588
Mo	0.97	0.99	0.9854	0.0069
Al	0.001	0.017	0.0117	0.0057
ε (%)	0.0500	5.0000	0.9609	1.4397

Table 5. Empirical input variables of the neural network model [26, 27].

A database was prepared for training of the empirical neural networks. All the data of inputs and output were randomized and split into a training set and a testing set. The procedure of training and testing the empirical model was the same as the physical creep strain model detailed discussed in previous sections. The normalized values of 12 inputs and the output were shown in Table 5.

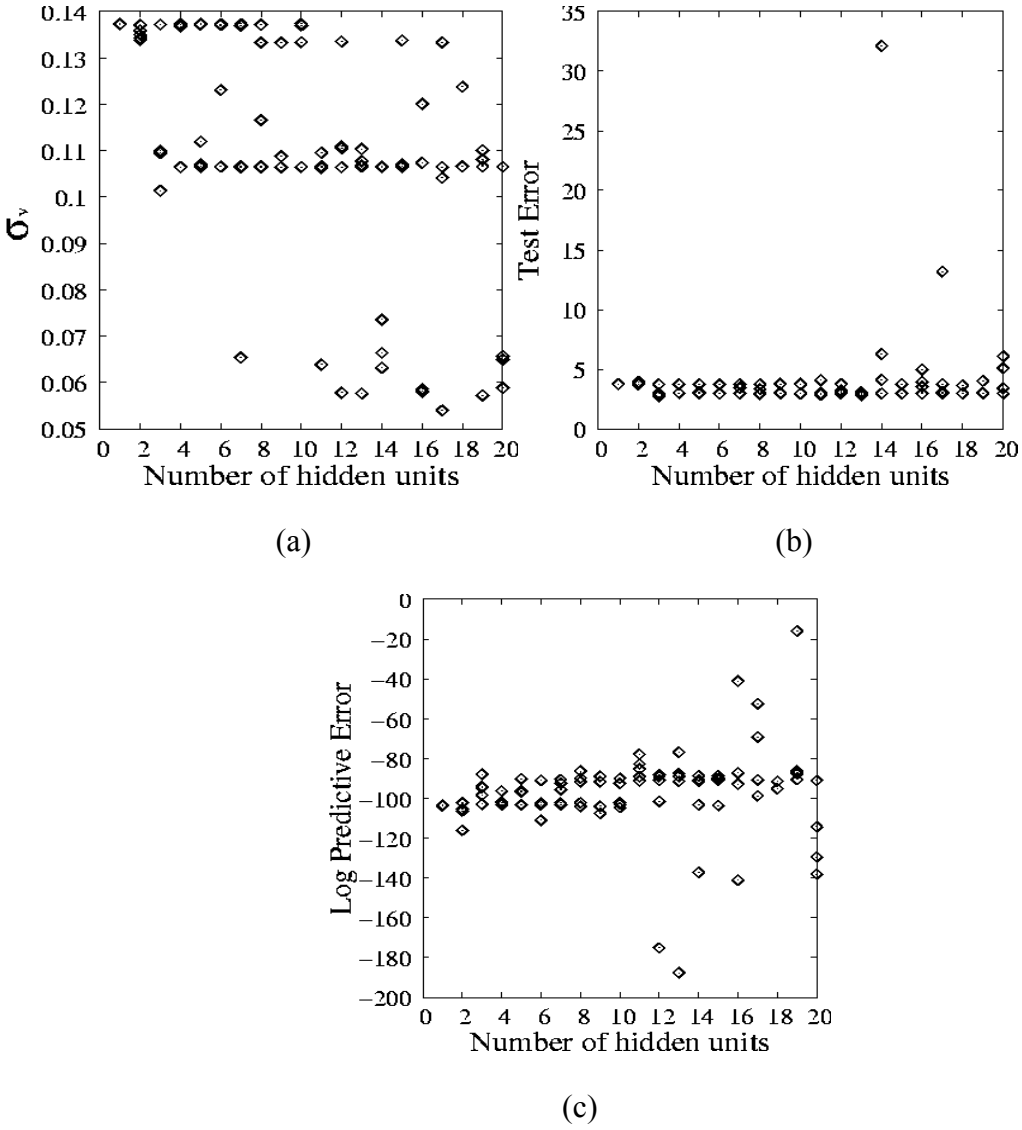

(a) (b)

(c)

Figure 3.4 The perceived level of noise σ_v (a), the test error (b) and the log predictive error (c) of empirical model with increasing numbers of hidden units.

As it showed in Figure 3.4, the perceived level of noise σ_v did not decreased as the number of hidden units increased. The log predictive error (LPE) nearly levelled out as the fitting function became more flexible with large number of hidden units.

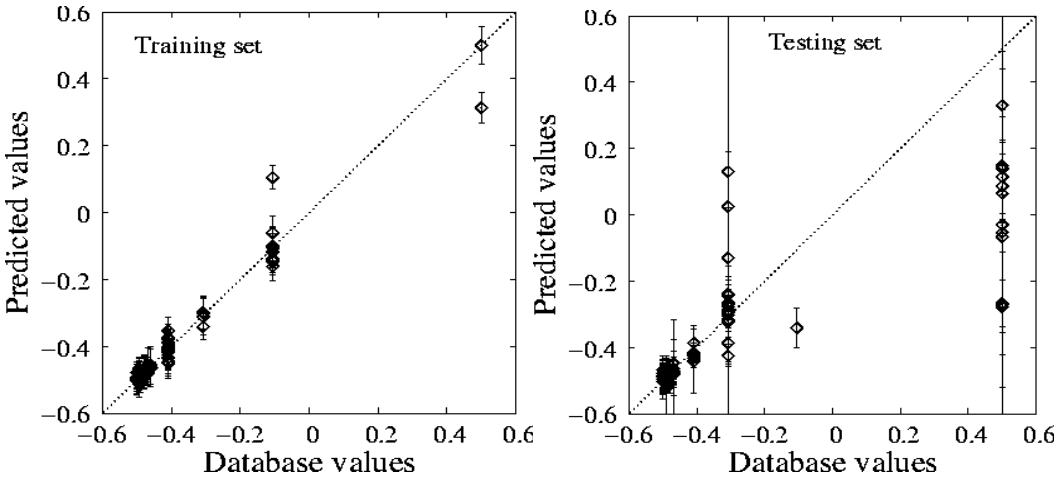

(a) (b)

Figure 4.4 Comparison of predicted versus actual creep strains for the training set (a) and testing set (b), using the best model.

Figure 4.4 shows the comparison of predicted versus actual creep strains for the training set (a) and testing set (b), using the best model. The predictions on the testing database (unseen data) by the neural network model show very poor agreement. Additional physical inputs were required in order to get more accurate non-linear relationship between the empirical inputs and the creep strain. Comparing the training data and testing data of the completely empirical model with the ones of the model using physical inputs, it is clear that the model with physical inputs (which has been discussed in detail in section 3.5) has better agreement with experimental data. And predictions with the physical strain model should be reliable.

Chapter 4

Results and Discussion

4.1 Prediction

A great number of predictions were made under different creep conditions (creep stress, time and temperature etc.) and for various steels. Since the two input variables $\frac{1}{T}$ and ln(T) were both dependent on the absolute temperature T, in the case of prediction, the variable $\frac{1}{T}$ was selected as the only one input variable varying when predicting the dependence of the output ln(ε) on the input, and the other variable ln(T) would vary automatically as the temperature T changed from its minimum to the maximum with the same step of the variable.

4. 2 Plots and analysis of the predictions

4.2.1 Predictions of ln(ε) versus $\frac{1}{T}$

When predicting the dependence of ln(ε) on the first input variable $\frac{1}{T}$, the variable ln(T) would vary automatically as the temperature T varies. And the other twelve input variables were set as the constant values associated with one of the specific 2.25Cr-1Mo steels, e.g. the chemical compositions and heat treatment methods were set to the steel of W1413. A large number of predictions were made, and some plots are shown below for detailed study.

When the temperature ranging from 700K to 900K in the case of prediction, the variable shear modulus G=-1.08×10^{-3}×T+8.87 could be regarded as a constant since the difference between G_{min} and G_{max} was quite small (G_{min}= 7.9×10^{10} N/m^2, when T= 900K; and G_{max}=8.114×10^{10} N/m^2, when T= 700K). In this prediction, when the only varying variable $\frac{1}{T}$ ranging from 0.0011 to 0.00125 (K^{-1}), the shear modulus could be regarded as a constant (G=8.006×10^{10} N/m^2 for T=800K), and the rest of the variables were set as constant values such as ln($\frac{\sigma}{G}$)=-7.3785 for stress σ=50MPa. And the chemical compositions were set as one of the particular steels.

As the plots of predictions had shown in Figure 4.1, a definite trend was evident that the output ln(ε) decreased as the input variable $\frac{1}{T}$ varied. In other words, creep strain ε was getting lower when the temperature T of the test steel varied from 909K to 800K at different stresses and for different creep time. It has long been known, the creep strain would increase as the temperature elevates, which means the predictions were reasonable theoretically.

When the predictions were made under the same stress σ=50MPa, the predicted value of the output variable ln(ε) augmented when the creep time t varied from 100h to 1000h, and 10000h, which could be seen from Figure 4.1 (a), (c) and (e). And the predictions at σ=70MPa had the same characteristics (shown in Figure 4.1 (b), (d), (f)). When the predictions were made for the same creep time (t=100h) but at different stresses (σ_1=50MPa, σ_2=70MPa), as shown in Figure 4.1 (a) and (b), at one particular

temperature, the value of $\ln(\varepsilon)$ with larger stress σ_2=70MPa (Figure 4.1 (b)) was greater than the one with smaller stress σ_1=50MPa (Figure 4.1 (a)).

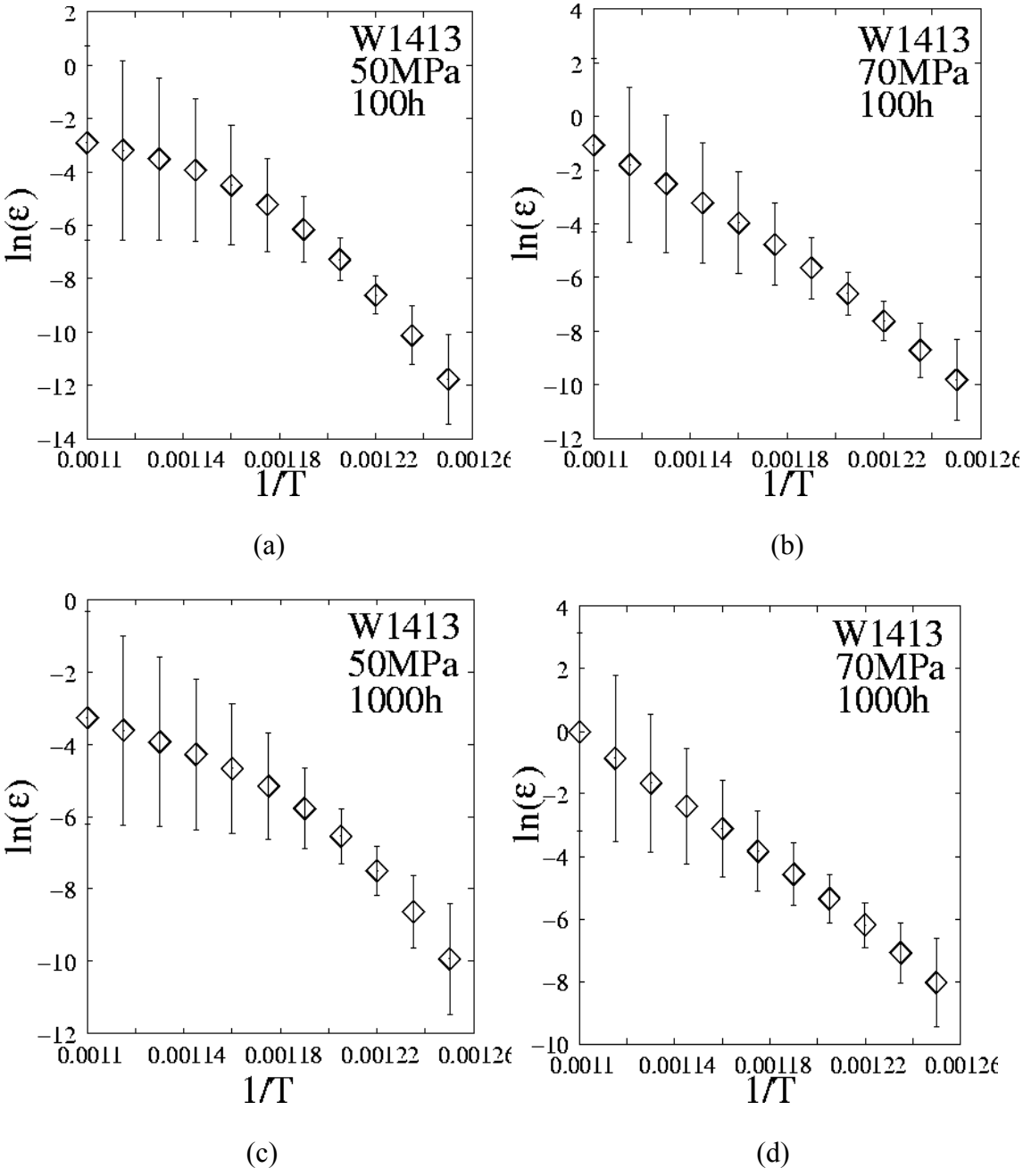

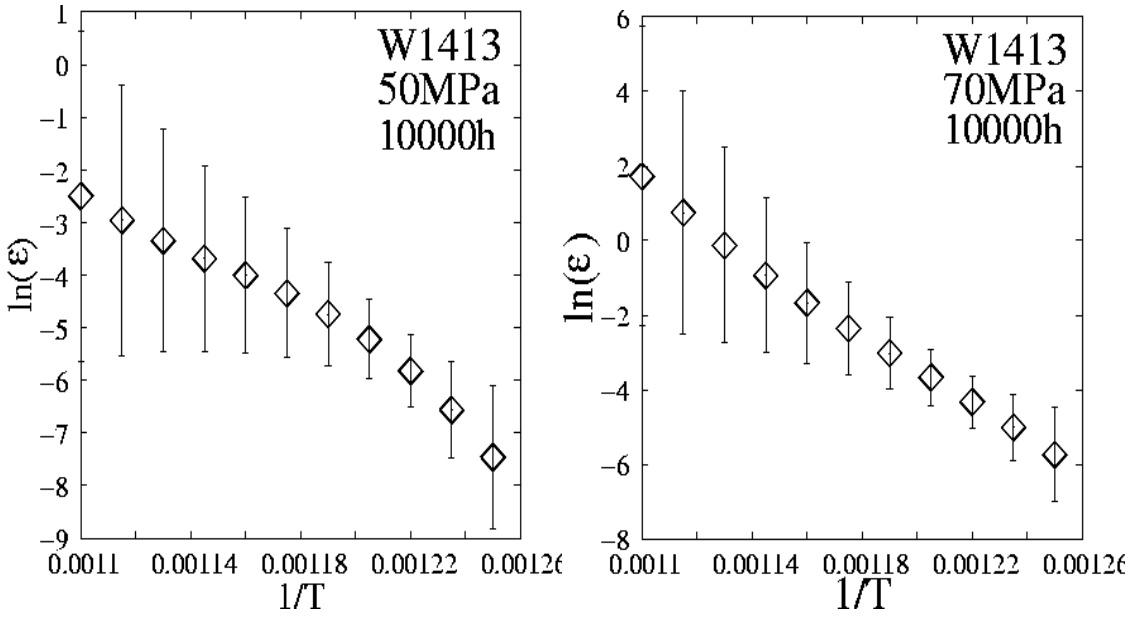

(e) (f)

Figure 4.1 Prediction of ln(ε) vs. 1/T for W1413 at different stress σ for different creep time t.

There were a lot of data on the creep strains at different stresses when T=823K, but the database lacked enough experimental data on strain under other temperatures. That was why the predictions in this area were more reasonable than others. The elastic strain at the yield strength is approximately ε=0.001 for a steel, which indicated the regions below ln(0.001)= –6.9 did not have physical sense because the strain values were very small (Figure 4.1). The creep curve of strain against time would stop at its rupture point (detailed analysis on strain against time would be shown next step).

The error bars of the plots in the predictions represented the uncertainty in fitting the non-linear function to the training data. And the error bars of the predicted values of ln(ε) were getting enormous when the input $\frac{1}{T}$ ranging from 0.0011 to 0.00116 (at the same

time, the temperature T elevated from 862K to 909K). It is clear that more additional experimental data under different temperatures should be included in the database of the neural network model in order to get more reliable predictions on creep strain.

The inverse of temperature made the plots of $\ln(\varepsilon)$ versus $\frac{1}{T}$ have a very clear picture of varying trend, but they were not easy to understand. Plots of $\ln(\varepsilon)$ against temperature shown in Figure 4.2 (a), and strain against temperature shown in Figure 4.2 (b) would express their relationship more clearly. The exact values of strain and temperature could be calculated with the data from the data file of previous predictions on $\ln(\varepsilon)$ versus $\frac{1}{T}$.

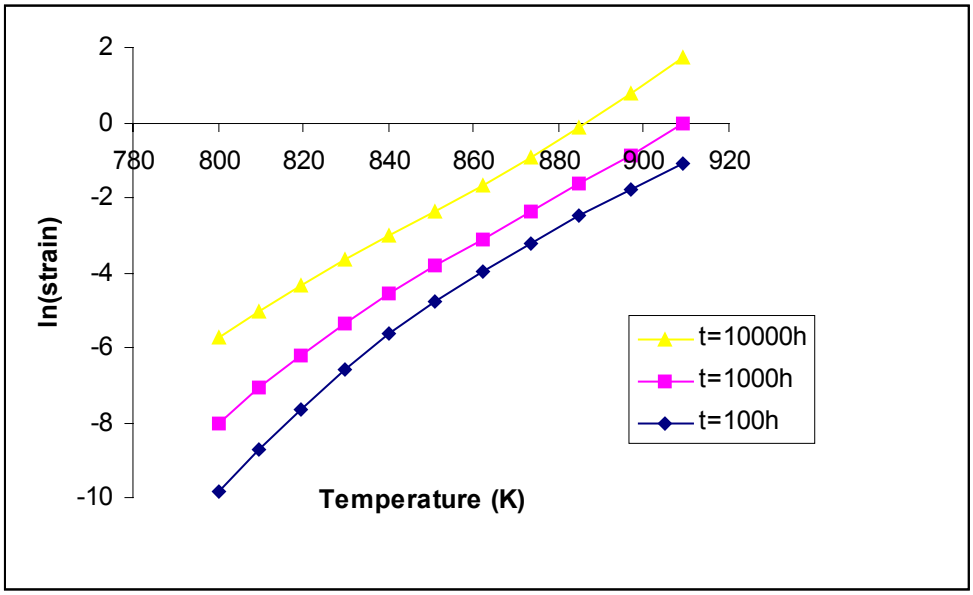

Figure 4.2 (a) Prediction of $\ln(\varepsilon)$ versus temperature of W1413 at σ=70MPa for different creep time.

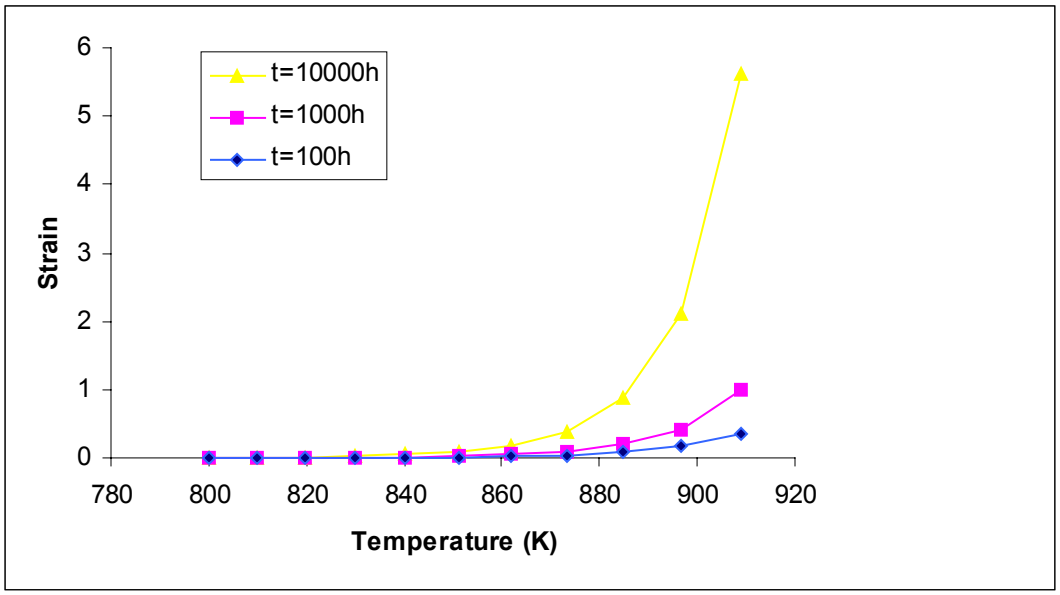

Figure 4.2 (b) Prediction of strain versus temperature of W1413 at σ=70MPa for different creep times.

As expected, Figure 4.2 (b) showed the creep strain increased its values as the temperature elevated from 800K to 900K. At the particular temperature, the longer the creep time lasted, the higher the strain value (e.g. at the particular temperature T=909K, the strain was ε=5.61 for the yellow curve when t=10000h). However, the steel would have ruptured before its strain value could reach that high value. In the original database of the neural network model, temperature was ranging from 673 to 833K.

A clear picture on strain against temperature would be available if the prediction was made when temperature ranging from 800 to 840K. As Figure 4.3 shows, the prediction was made at σ=70MPa and t=1000h for steel W1413. The error bounds shown in Figure 4.3 indicate the uncertainty of the prediction on strain against temperature. The error bounds expanded as the temperature approached T= 850K, and the uncertainty of

prediction also increased. The error bounds were quite small when the prediction temperature ranging from 800K to 830K because there were a lot of creep data of steel at T=823K in the original database, which made the prediction of this region more accurate.

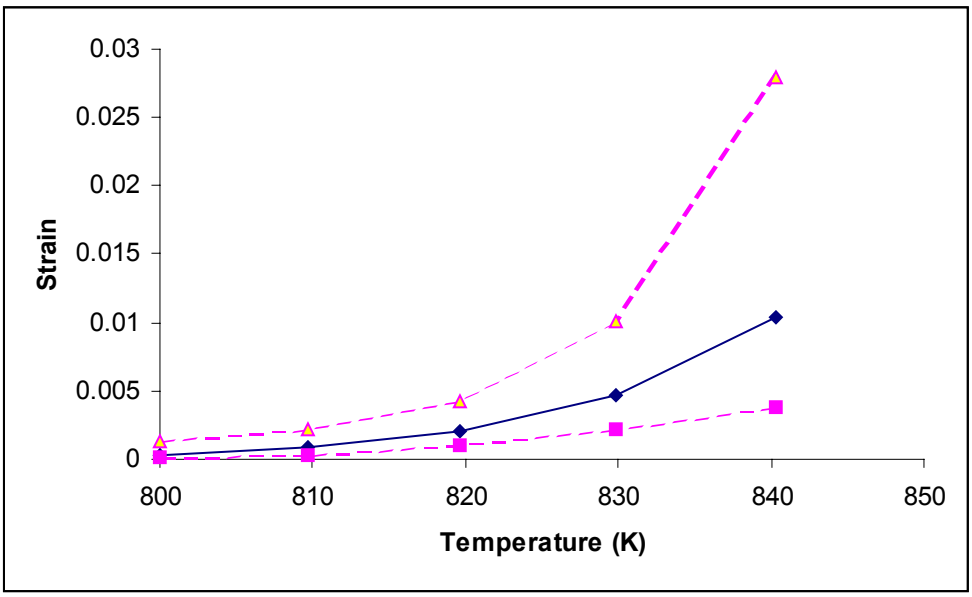

Figure 4.3 Prediction of strain with error bounds against temperature at σ=70MPa and t=1000h for W1413.

4.2.2 Predictions of $\ln(\varepsilon)$ versus $\ln(\frac{\sigma}{G})$

In this case of prediction, the target was the natural logarithm of creep strain $\ln(\varepsilon)$, and the varying input was $\ln(\frac{\sigma}{G})$. Figure 4.4 illustrated the predicted effect of the input variable $\ln(\frac{\sigma}{G})$ on the creep strain $\ln(\varepsilon)$ for the composition of W1420 steel. The shear modulus was also set as a constant G=8.006×10^{10} N/m^2 at the temperature T=800K. The

stress was allowed to vary from 70MPa to 200MPa, and the $\ln(\frac{\sigma}{G})$ ranged from –7 to –6 in the prediction.

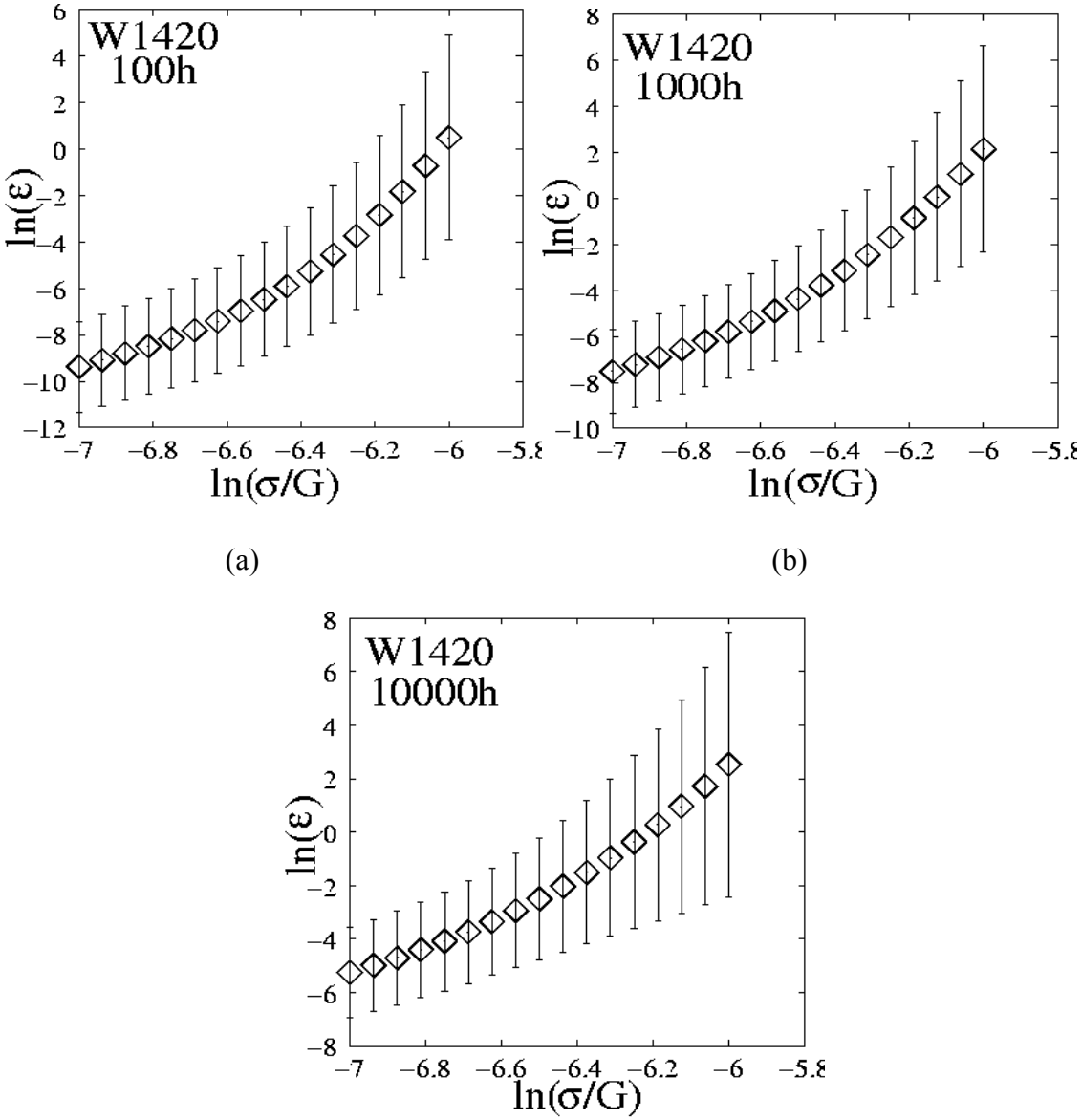

(a) (b)

(c)

Fig 4.4 Prediction of ln(ε) against $\ln(\frac{\sigma}{G})$ for W1420 for different creep time *t*.

It was obvious to see that the prediction of ln(ε) increased as the input ln($\frac{\sigma}{G}$) enlarging from the minimum to its maximum (in this case, the stress increased from 70MPa to 200MPa). Comparing the Figure 4.4 (a), (b) with (c), under the same stress (when the values of the input ln($\frac{\sigma}{G}$) were same), the prediction of the target ln(ε) would increase when the creep time was getting longer from 100h to 10000h.

4.2.3 Predictions of ln(ε) versus ln(t)

According to the perceived significances value σ_w, the input variable of ln(t) is very important for the prediction of ln(ε). Several predictions were made using data of various steels and under different stress and temperature conditions. Two of the predictions samples were focused on for detailed study (Figure 4.5).

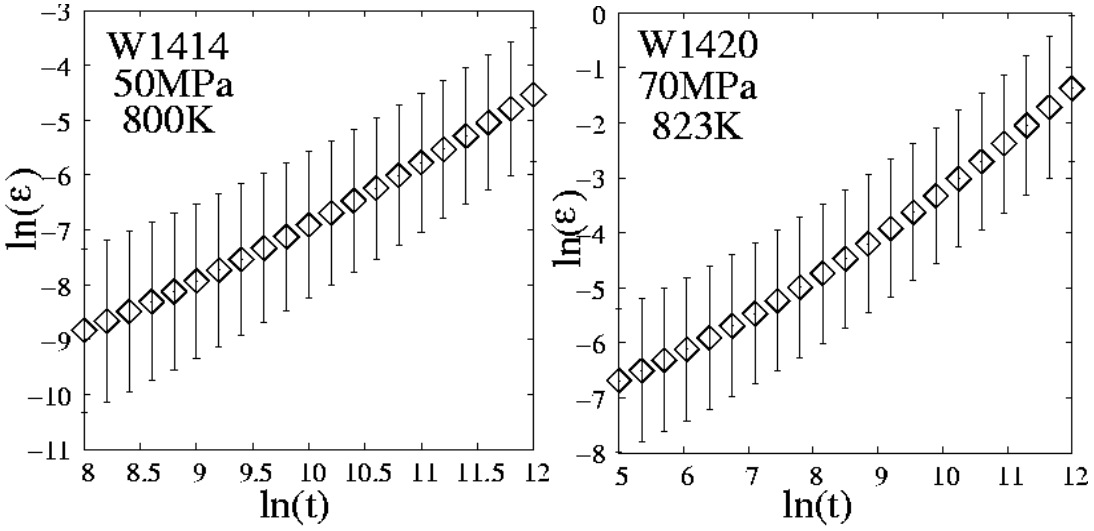

(a) (b)

Figure 4.5 Predictions of ln(ε) against ln(t) for various steels at different creep conditions.

A definite trend was evident that the prediction of ln(ε) increased as the input ln(t) extended until the creep rupture point. Some real experimental creep test data were used to test whether the prediction of the model was reasonable or not. Creep data were collected from reference and published literatures, and the creep strain should be less than 0.02 (ε<0.02) after 30 years testing (t=262800h).

Several predictions were made with the same creep conditions (creep stress and temperature) as the real experiments. For instance, the steel W1473 was selected to make a creep test when σ=100MPa and T=838K. In the case of the prediction, the conditions of composition were set to W1473. The temperature and stress were the same as the experiment: T=838K, σ=100MPa. And the maximum value of the input would be ln(t)=ln(262800)=12.48.

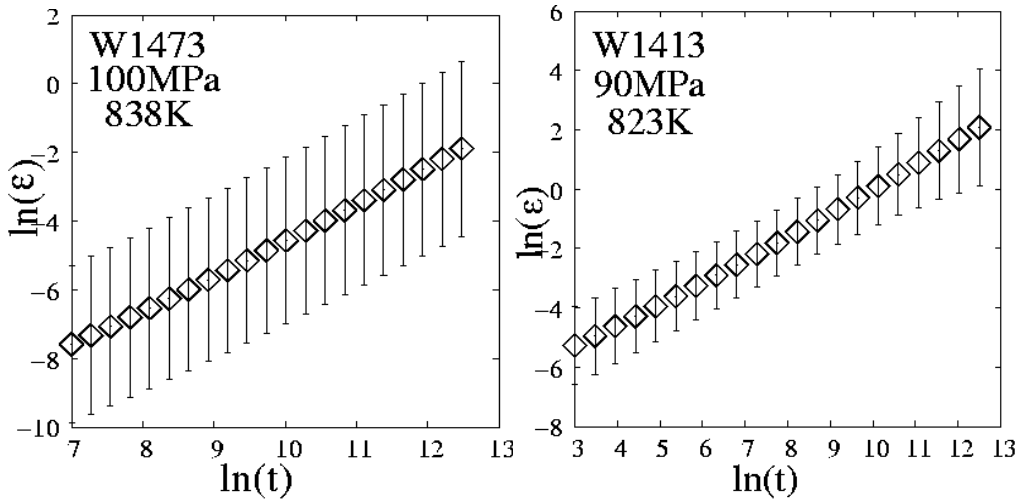

(a) (b)

Figure 4.6 Prediction of ln(ε) against ln(t). (a) for W1473 with the same creep conditions as the experiments. (b) for W1413 with different stress and temperature.

As expected, the output ln(ε) increased as the creep time extended. A detailed analysis on prediction data file stated that the maximum of target was ln(ε)=-1.533 when the input

ln(t)=12.8. In this case, the creep strain would be ε=0.21 when creep time t=362217h under the conditions of predictions.

However in the real experiment of creep test, the creep curve of strain against time would stop at its rupture point. It is believed that the steel will fail under the conditions of T=838K and σ=100MPa before the creep strain gets its ideal maximum value ε=0.21. Actually it ruptured when the strain was ε=0.003 and the creep rupture time was t=1995h, which could be calculated and predicted with a creep rupture model. More details of the methods and analysis on the prediction of creep rupture are given as below.

4.2.4 Predictions of ln(ε) versus C wt%

From the chart of model perceived significance for each input variables (Figure 3.3), the composition of carbon is also an important input for the prediction of the creep strain model. Predictions of ln(ε) dependence on the weight percent of carbon in the steel were made for different kind of 2.25Cr-1Mo. Two samples of prediction for steel of W1413 were shown as below (Figure 4.7). In this case, the variable shear modulus was regarded as a constant G=8.006×10^{10} N/m^2 when the temperature was set to its average value T=800K. As expected, when creep time changed from 100h to 1000h, under the same stress σ=100MPa, the prediction of ln(ε) would increased from ln(ε)=-3.5 to ln(ε)=-2 when the element of carbon was equal to 0.07 wt% (as shown in Figure 4.7 (a), (b)). And the creep strain decreased as the carbon weight percent (C wt%) increased.

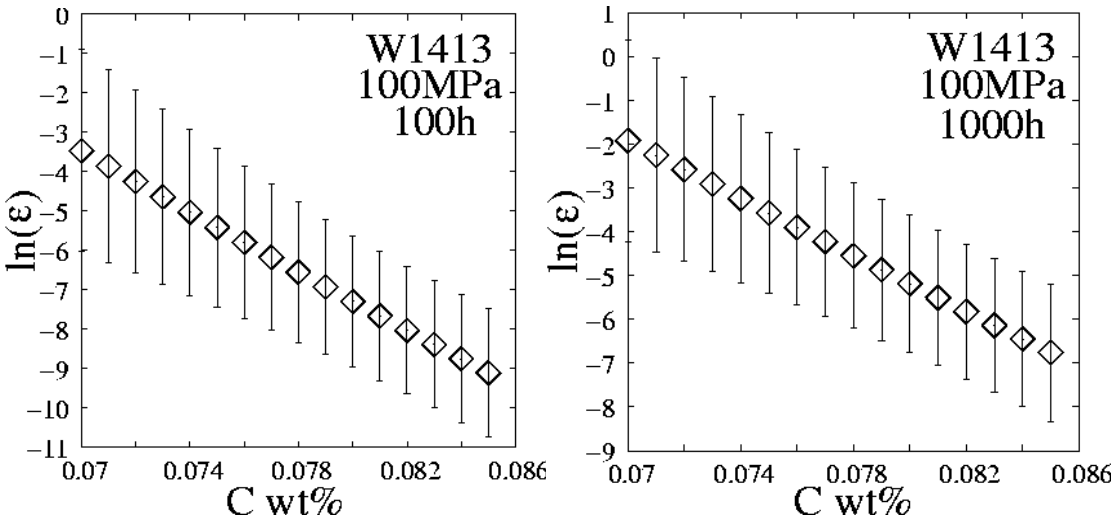

(a) (b)

Figure 4.7 Prediction of ln(ε) against the weight percent of carbon (C wt%) in the steel for W1420 at the same stresses for different creep time *t*.

The above phenomenon can be explained by micro-structural theory. It is believed that the increasing of the carbon (C wt%) would lead to the formation of precipitate in the steel, which results in the strength value of the steels getting larger. As a matter of fact, the creep strain will decrease as the weight percent of carbon increases in the steels.

4.3 Prediction of strain versus time

4.3.1 The prediction of creep rupture life of 2.25Cr-1Mo

The rupture life predictor could predict the rupture life of the steel under the particular creep conditions. For example, the predictions of rupture life of 2.25Cr-1Mo for different temperature were shown in Figure 4.8. Rupture was predicted to occur after 1995h for a stress of 100MPa, e.g. rupture life of 2.25Cr-1Mo would be $t=10^{3.3}$=1995h at the stress σ=100MPa in Figure 4.8 (a). In this prediction, the creep strain was

ε=0.003. The creep strain of 2.25Cr-1Mo steel should be less than 0.02 (ε<0.02) after it had been operated for 30 years (t=262800h) at σ=100MPa and T=838K. In the present of prediction, the creep strain ε=0.003 is smaller than 0.02, which means the predictions were reasonable.

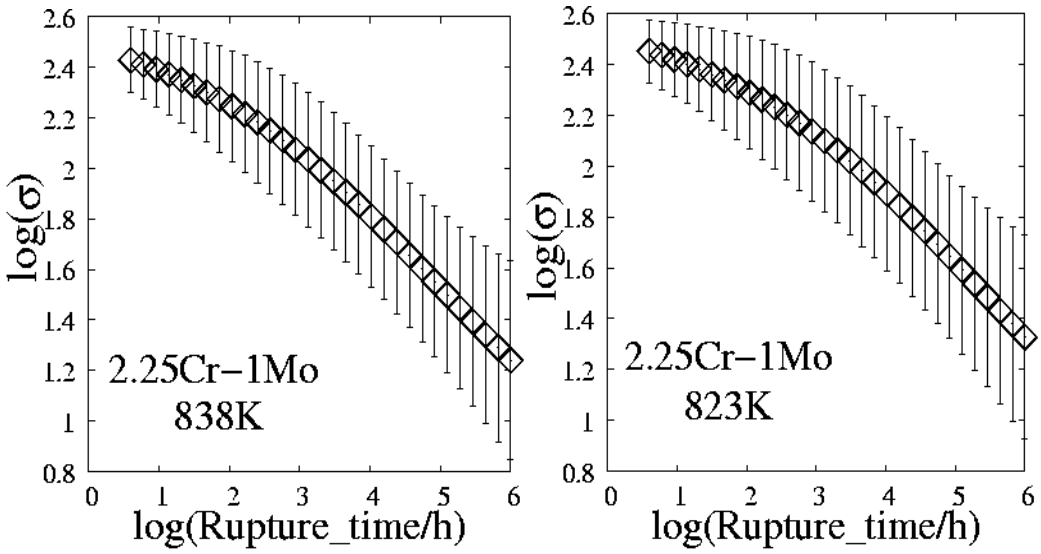

(a) (b)

Figure 4.8 Prediction of the rupture life of 2.25Cr-1Mo under different temperature.

Another sample of creep rupture life was made as shown in Figure 4.8 (b). The rupture life was t> 15848h as calculated when creep stress σ=70MPa and the temperature T=823K in the prediction model. The real experimental data could be collected from the reference [27], in which the creep rupture life was t=18384h when σ=70MPa and T=823K. It would prove the prediction model of rupture life was reliable.

4.3.2 The prediction of W1420 steel

A curve of creep strain against creep time could be obtained with the data file of the prediction of ln(ε) against ln(t) (as Figure 4.6 (b) shown). The rupture time could be calculated with the rupture prediction model, the steel W1420 would rupture when

t=15848h at the creep tested under the conditions of σ=70MPa and T=823K. And the creep strain would be ε=0.0316 when the rupture occurred according to the present prediction (Figure 4.9).

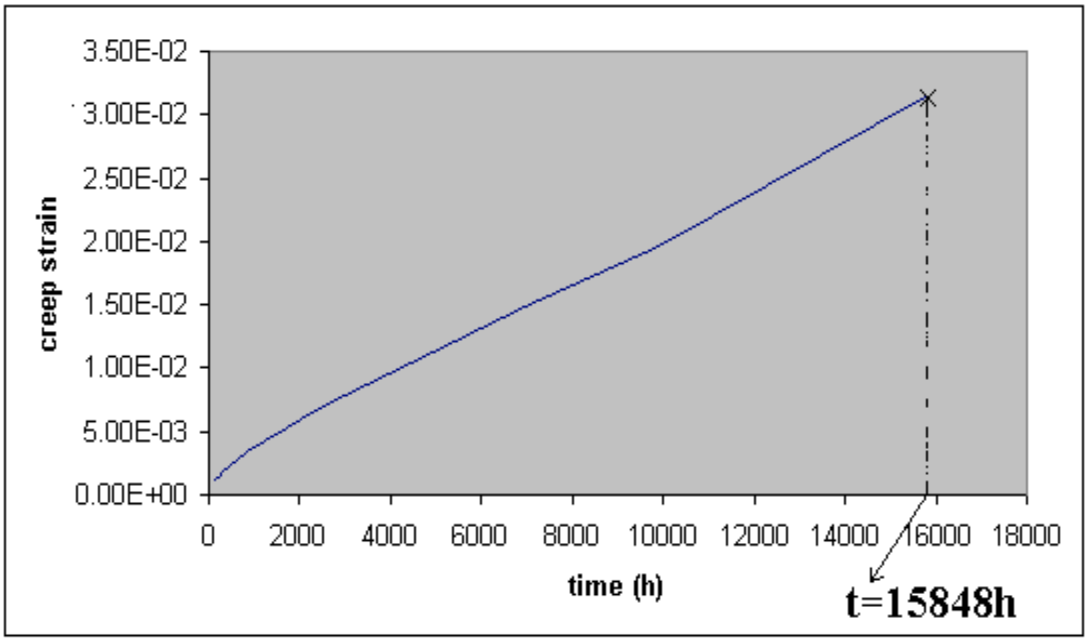

Figure 4.9 Prediction of creep strain against the creep time for W1420 at T=823K, σ=70MPa. It would rupture at the point when t=15848h

4.4 Three dimensional plot of prediction

The neural network strain model could make a non-linear relationship between the output and inputs. For example, a lot of predictions of $\ln(\varepsilon)$ against $\frac{1}{T}$ at different stresses were made. In this case of prediction, the compositions were set as a particular steel (e.g. W1414), and the creep time was t=100h. When the temperature ranging from 750K to 840K, twenty predictions were made in which the stress was ranging from σ_1=30MP to σ_{20}=220MPa (the varying step of the stress is σ=10MPa). Data of

predicted ln(ε) and two variables $\frac{1}{T}$ and stress σ were collected to make a three dimensional graph of ln(ε) versus T, σ (as shown in Figure 4.10). It is obvious that the predicted ln(ε) is a non-linear function of temperature and stress. The predicted values of ln(ε) increased as the temperature elevated and the stress increased.

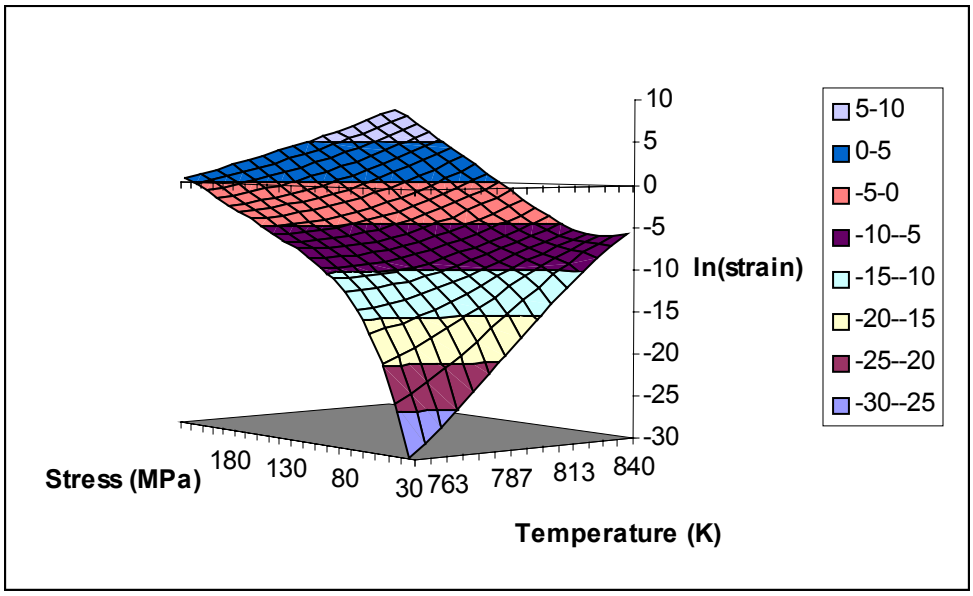

Figure 4.10 Three-dimensional plot of ln(ε) against stress and temperature for W1414 at t=100h.

When the temperature was low and the stress was small, i.e. at T=770K and σ=40MPa, the predicted value ln(ε)= -20.55, therefore the strain ε=1.2×10^{-9}, which is very small. However, as the temperature and the stress increased, i.e. when T=826K and σ=90MPa, the predicted ln(ε)= -5.54 and ε=0.39%. The experimental creep data at the similar conditions could be found in literature [41], the strain ε=0.38% when T=826K, t=100h and σ=90MPa.

Chapter 5

Summary and Future Work

Considerable work has been published on modelling the creep rupture rather than creep strain, because the creep rupture stress and rupture life are more useful than creep strain in designing alloy components.

The aim of the present work was the study of the creep strain and the constitutive equations. The creep strain and its dependence for a selected steel 2.25Cr-1Mo have been analysed using a neural networks method within a Bayesian framework. The model was based on a large data set accumulated from the literature. The data were obtained from a variety of sources and cover a wide range of compositions and heat treatments of 2. 25Cr-1Mo steels.

A neural network model of creep strain based on a sample constitutive equation was created to study the influence of stress, temperature, time, chemical compositions and heat treatment conditions on creep strain of 2.25Cr-1Mo steels. A lot of predictions of creep strain on various inputs at different creep conditions were made and the model successfully predicted the strain varying with time in a particular range of input variables.

However, the error bars of the prediction was extending when extrapolating the prediction on a wide range of inputs. The reason why the predictions were reasonable only in a narrow range was due to the weakness of the neural network models. The neural network model needs a great number of data on a wide range of inputs in order to create more accurate predictions. However, creep strain data are generally kept secretly for commercial reasons and it is quite difficult to find general data for creep strain. In the case of creep strain model, there were only seven types of 2.25Cr-1Mo steels available in

Table 2; and the temperature ranged from 666K to 823K, which was a quite limited range for the empirical neural network models.

Generally, the prediction of strain against the creep time was on the secondary stage of creep curve (also known as the steady-state stage). The minimum of creep strain would be the value of elastic strain when the steel 2.25Cr-1Mo was tested at the condition of T=838K and σ=100Mpa. When the power plant components made of 2.25Cr-1Mo steel worked for 30 years, the strain value would be no greater than 2% (ε<0.02).

The dependence of strain on stress, time, and temperature was discussed for steady state of creep deformation under uni-axial loading at different constant temperatures. Only the primary and secondary stages of creep were studied in this dissertation because the tertiary stage is closely related to fracture. The creep rupture points of 2.25Cr-1Mo steel at specific stress and temperature could be predicted with the creep rupture model, and the predictions of rupture life fitted the experimental data quite well.

Although the aim of the research project behind this thesis has been fulfilled with the work presented, there are some aspects that could lead to improvements in the models presented. It is clear from the previous analysis on the predictions that much more additional experimental creep data of various temperatures and for different steels were required in the vast database in order to get a more reliable and accurate prediction of neural network in which physical models were inputs. Once the neural network with physical models as inputs was built on the basis of a database containing a large number of creep data, more reasonable and accurate predictions could give a clear picture of creep strain and its dependence.

Reference

1. H. E. Evans *Mechanisms of Creep Fracture*, Elsevier Applied Science Publishers, London and New York (1984) 1-22.

2. R. W. Evans and B. Wilshire, *Introduction to Creep*, The Institute of Materials, London (1993) 1-75.

3. C. D. Pomeroy, *Creep of Engineering Materials*, Mechanical Engineering Publications Limited, London (1978) 85-110.

4. *Glossary of Materials Testing Terms* www.instron.com/apps/glossary/c.asp

5. J. Cadek, *Creep In Metallic Materials,* Institute of Physical Metallurgy of the Czechoslovak Academy of Sciences, Brno, Czechoslovakia (1988) 13-29.

6. M. Murugananth, *Design of Welding Alloys for Creep and Toughness*, PhD Thesis, University of Cambridge (2002) 15-54

7. J. L. Rhoads *Basic Explanation of Creep Process,* http://www.nuc.berkeley.edu/thyd/ne161/jlrhoads/creep.html

8. U. Martin, U. Mühle and H. Oettel, *Computational Materials Science* **9** (1997) 92-98.

9. F.C. Monkman and N. J. Grant, *Proc. ASTM* **56** (1956) 593.

10. C. Phaniraj, B. K. Choudhary, K. Bhanu Sankara Rao and Baldev Raj, *Scripta Materialia,* **48**, Issue 9 (2003) 1313-1318.

11. R. W. Evans and B. Wilshire, *Creep of Metals and Alloys,* The Institute of Metals, London (1985) 1-104.

12. H. K. D. H. Bhadeshia, *Mechanisms and Models for Creep Deformation and Rupture,* 1-38 unpublished work

13. K. Maruyama, H. Kushima and T. Watanabe, *Prediction of Long Term Creep Curve and Rupture Life of 2.25Cr-1Mo Steel,* ISIJ International, Vol. 30 (1990) 817-822.

14. K. Maruyama and H. Oikawa, *Trans ASME*, *J. Pressure Vessel Technology*, **109** (1987) 142.

15. K. Maruyama, C. Harada and H. Oikawa, *Trans. Iron Steel Inst.* Japan, **26** (1986) 212.

16. D. J. C. Mackay, *Bayesian Non-linear Modelling with Neural Networks,* eds H. Cerjak and H. K. D. H. Bhadeshia, The Institute of Materials, London (1997) 359-389

17. D. J. C. Mackay, *Neural Computation*, **4** (1992a) 415-447.

18. D. J. C. Mackay, *Neural Computation*, **4** (1992b) 448-472.

19. H. H. D. H. Bhadeshia, D. J. C. Mackay and L. E. Svensson, *Baysian Neural Network Modelling of Weld Toughness,* Materials Science and Technology, (1995)

20. T. Cool, H. K. D. H. Bhadeshia and D. J. C. Mackay, *Modelling The Mechanical Properties in The Haz of Power Plant Steels I: Bayesian Neural Network Analysis of Proof Strength,* eds H. Cerjak and H. K. D. H. Bhadeshia, The Institute of Materials, London (1997) 403-442.

21. H. K. D. H. Bhadeshia, *ISIJ International* **39** (1999) 966-979.

22. D. Cole. C. Martin-Moran, A. G. Sheard, H. K. D. H. Bhadeshia and D. J. C. MacKay, *Modelling Creep Rupture Strength of Ferritic Steel Welds,* Science and Technology of Welding and Joining, Vol. **5** (2000) No.2 81-89.

23. T. G. Langdon, *Dislocations and Properties of Real Materials,* Institute of Metals, London (1985) 221-238.

24. H. K. D. H. Bhadeshia, *Modelling of Microstructureal Evolution in Creep Resistant Materials,* eds K. Easterling and H. Cerjak, The Institute of Materials, London (1998) 109.

25. J. Kučera, *Czech. J. Physics* **B29** (1979) 797-809.

26. National Research Institute for Metals: NRIM *Creep Data Sheets*, 1997, 11B 1-20.

27. *The Creep and Creep Rupture Properties of 2.25Cr-1Mo Weld Metals*, NEI PARSONS Limited, (1980) 1-20

28. W. Köter, *Arch. Eisenhüttenw.,* 1940, Vol. **6**, 271-278

29. W. Köter and H. Franz, *Metals Rev.,* 1961,Vol. **6**, 1-55

30. G. R. Speich, A. J. Schwoeble, W. C. Leslie, *Elastic Constants of Binary Iron-Base Alloys, Metallurgical Transactions,* **3** (1972) 2031-2037.

31. T. Sourmail, H. K. D. H. Bhadeshia and D. J. C. Mackay, *Neural Network Model of Creep Strength of Austenitic Stainless Steels,* Materials Science and Technology, Vol. **18,** 655-663.

32. D. J. C. Mackay, *Neural Computation*, **4** (1992c) 698.

Materials Algorithms Project

Program Library

Program MAP_STEEL_FERRITIC_CREEP_RUPTURE

1. Provenance of code.
2. Purpose of code.
3. Specification.
4. Description of program's operation.
5. References.
6. Parameter descriptions.
7. Error indicators.
8. Accuracy estimate.
9. Any additional information.
10. Example of code
11. Auxiliary routines required.
12. Keywords.
13. Download source code.
14. Links.

Provenance of Source Code

Murugananth M
Phase Transformations Group,
Department of Materials Science and Metallurgy,
University of Cambridge,
Cambridge CB2 3QZ, U.K.

The neural network program was produced by:

David MacKay,

Cavendish Laboratory,

University of Cambridge,
Madingley Road,
Cambridge, CB3 0HE, U.K.
E-mail: Murugananth

Added to MAP: May 2002.

Top | Next

Purpose

To predict the Creep Rupture Strength of plates and welds.

Top | Next | Prev

Specification

Language: C,FORTRAN, Shell script
Product form: Source code / executables
Platform : Solaris, Linux

Complete program.

Top | Next | Prev

Description

A program for the estimation of the creep life of ferritic steels as a function of elemental composition, test conditions and solution treatment.

Description of the files and their usage in the present module :

Readme	Tells the name of the input variables and the order in which these are to be presented in a file named anndata_example before using the model for predictions.
anndata_example	A file having the base composition of the alloy that is to be analysed. "example" is the identification of the alloy here. And the file name from which test.dat is generated. One can resonably modify this file to step as many variables as there are. The format of this file is [base composition] [minimum] [maximum] [step] [1(=step) or 0 (=use value from base comp)] [variable name]
RESULT_example	Directory where the predicted results of an alloy with identification name "example" can be found.
run	This file has to be used to predict. Either execute it with the command "csh run" or "./run". This would take you through all the processes and at the end will let you know the place where your results can be located.

Directory "bin"	
MINMAX	Contains the minimum and maximum ranges of each input variable.
test.dat	Contains the input variables which will be used by accessory programs to make predictions.
data_no.c	A C-file to get the number of data in test.dat file via keyboard input.
predict	A file containing the shell commands.
generate44	This is the executable file for the neural network program. It reads the normalised input data file, norm_test.in, and uses the weight files in subdirectory c, to find a value for ferrite number.The results are written to the temporary output file _out.
spec.c	Specification file to be read by generate44.
_ot, _out, _res, _sen	These files are created by generate44 and can be deleted.
Directory sbin	
Agen_data_tmp	To step the variables which are denoted in the file "anndata_example"
Aget_result	To split the results if many variables are varied simultaneously
log	To log or anitlog the results from predictions.
c	Directory where weight files for use by the generate44 pertaining to each model in the committee are stored.
d	Directory where the normalised values of inputs and output are stored
outprdt	Directory where the output from generate44 are written to.
DIRECTORY s	
committee.dat	Consists of values representing the number of models in committee and number of variables used.
normtest.for	Program to normalise the input data read from test.dat. Also produces the normalised input file norm_test.in. It makes use of information read in from no_of_rows.dat and committee.dat.
gencom.for	This program uses the information in committee.dat and combines the predictions from the individual models, in subdirectory outprdt, to obtain an averaged value (committee prediction). The output (in normalised form) is written to com.dat.
treatout.for	Program to un-normalise the committee results in com.dat and write the output predictions to unnorm_com. This file is then renamed as result.

Instructions to run the module

- Download the module according to your requirement (Unix or Linux platform)
- gunzip the module using the command "gunzip creep_model_Linux.tar.gz "
- untar the file using "tar -xvf creep_model_Linux.tar"
- Change directory to either creep_model_linux (or) creep_model_unix
- Rename or copy anndata_example file and modify it according to your requirements (follow instructions in the above table to modify).
- To execute type ./run or csh run at the command prompt
- Follow the instructions given then

Top | Next | Prev

References

1. D. G. Cole, C. Martin-Moran, A. G. Sheard, H. K. D. H. Bhadeshia and D. J. C. MacKay, 1999, *Science and Technology of Welding and Joining*, Accepted for publication.
2. D.J.C. MacKay, 1997, *Mathematical Modelling of Weld Phenomena 3*, eds. H Cerjak & H.K.D.H. Bhadeshia, Inst. of Materials, pp 359.
3. D.J.C MacKay's website at http://wol.inference.phy.cam.ac.uk/mackay/README.html#Source_code

Top | Next | Prev

Parameters

Input parameters

- log(Rupture time / h)
- Temperature / K
- Carbon / wt%
- Silicon / wt%
- Manganese / wt%
- Phosphorus / wt%
- Sulphur / wt%

- Chromium / wt%
- Molybdenum / wt%
- Tungsten / wt%
- Nickel / wt%
- Copper / wt%
- Vanadium / wt%
- Niobium / wt%
- Nitrogen / wt%
- Alumimium / wt%
- Boron / wt%
- Cobalt / wt%
- Tantalum / wt%
- Oxygen / wt%
- Rhenium / wt%
- Normalising Temperature / K
- Normalising Time / h
- Cooling rate of normalise in air or furnace (0 or 1)
- Cooling rate of Normalise in air(0 or 1)
- Cooling rate of Normalise for oil quench (0 or 1)
- Cooling rate of Normalise for water quench (0 or 1)
- Tempering Temperature / K
- Tempering time / h
- Cooling rate of Temper in furnace (0 or 1)
- cooling rate of Temper in air (0 or 1)
- Cooling rate of Temper for oil quench (0 or 1)
- Cooling rate of Temper for water quench (0 or 1)
- Annealing temperature / K

- Annealing Time / h
- Cooling rate of anneal in furnace (0 or 1)
- Cooling rate of anneal in air (0 or 1)

Output parameters

Directory having the result files with format predictions,predictions-error, predictions+error

Top | Next | Prev

Error Indicators

None.

Top | Next | Prev

Accuracy

No information supplied.

Top | Next | Prev

Further Comments

None.

Top | Next | Prev

Example

1. Program text

Complete program.

2. Program data

See file anndata_example

3. Program results

Refer example file in example directory : RESULT_example

Top | Next | Prev

Auxiliary Routines

None

Top | Next | Prev

Keywords

Creep Rupture Strength, Power plant steels, Chromium steels

Download source code

- Linux platform (version 1.1)
- Unix platform (Sun OS)(version 1.1)

(Download the files according to the platform Unix or Linux and then gunzip <filename> followed by tar -xvf <filename>)

MAP originated from a joint project of the National Physical Laboratory and the University of Cambridge.
